Catalysis Today 147S (2009) S305–S312

Contents lists available at ScienceDirect

Catalysis Today

journal homepage: www.elsevier.com/locate/cattod

Effect of structure and thermal properties of a Fischer–Tropsch catalyst in a fixed bed

Régis Philippe [a,*], Maxime Lacroix [b], Lamia Dreibine [b], Cuong Pham-Huu [b], David Edouard [b], Sabine Savin [c], Francis Luck [d], Daniel Schweich [a]

[a] Laboratoire de Génie des Procédés Catalytiques (LGPC) UMR 2214 CNRS/CPE Lyon, Université de Lyon, 43 boulevard du 11 Novembre 1918, 69616 Villeurbanne Cedex, France
[b] Laboratoire des Matériaux, Surfaces et Procédés pour la Catalyse (LMSPC), UMR 7515 CNRS/ECPM, Université Louis Pasteur, 25, rue Becquerel, 67087 Strasbourg Cedex 02, France
[c] Total E&P, Centre Scientifique et Technique Jean Feger, Avenue Larribeau, 64000 Pau, France
[d] TOTAL S.A., Direction Scientifique, 2 place de la Coupole, 92078 Paris La Défense Cedex, France

ARTICLE INFO

Article history:
Available online 8 August 2009

Keywords:
Catalyst support
Thermal effects
Fischer–Tropsch
Heat exchanges
Catalytic foam

ABSTRACT

A 2D G-S pseudo-homogeneous steady-state plug flow, non-isobaric and non-isothermal model is used to investigate the effects of operating conditions and catalyst thermal properties on the behaviour of a multi-tubular fixed bed for Fischer–Tropsch synthesis. This simulator allows observing, quantifying and discussing the influences of the gas velocity, the tube diameter, the type of catalyst used (monolithic foam or extrudates) and the heat conductivity of the support (alumina or silicon carbide). The observed responses are the effective thermal parameters of the catalytic bed, the radial and axial temperature profiles and the global performances of the reactor (yield, productivity and selectivity). Thermal properties of the support exhibit a strong influence when low fluid velocities and/or large tube diameters are employed. Because of the high void fraction of a foam structure these effects are less pronounced than with packed beds. This structural difference allows a wider range of operating conditions in terms of fluid velocity and tube diameter but underlines the necessity to tune the void fraction of a foam bed to obtain the best compromise between its volumetric catalytic activity and a good thermal behaviour.

1. Introduction

1.1. Background

Fischer–Tropsch synthesis (FTS) is a well-known catalytic reaction that yields synthetic fuels from a mixture of CO and H_2 obtained from coal (CTL process), natural gas (GTL process) or biomass (BTL process). Due to the global increase in energy costs, this reaction has known a renewed industrial and academic interest for approximately two decades [1,2]. The main products of FTS are paraffinic waxes based on the following global equation:

$$n{\cdot}CO + (2{\cdot}n + 1) \cdot H_2 \rightarrow C_nH_{2n+2} + n{\cdot}H_2O \quad (1)$$

The exothermicity encountered with FTS ($\Delta H = -165$ kJ/mol$_{CO}$ consumed) and the moderate range of catalytic activity are determinant parameters that dictate the choice of the reactor. High heat removal capacity and operation with the highest amount of catalyst (per unit volume of reactor) are necessary. An efficient heat removal is of crucial importance because too high hot spots may lead to a loss in selectivity, rapid deactivation of the catalyst and possible thermal runaways. Multi-tubular fixed bed reactors appear to be a possible technology. To be operated correctly and safely, the coupling between reaction, hydrodynamics and heat exchanges needs to be well understood. It is the aim of the present study.

1.2. Evaluation of the thermal constraint of the FTS

The evaluation of the thermal severity due to the FTS is approached with Mears criterion [3]. This later involves a comparison between the heat generated by the reaction and the ability of the catalytic bed to transfer heat away from the reaction zone towards the tube wall. It takes the form of Eq. (2). When this criterion is fulfilled, it can be assumed that the radial temperature profile is almost flat. This means that the reaction heat is rather well evacuated radially, however this does not ensure that there is no large hot spot along the bed:

$$(1-\varepsilon) \cdot r_p \cdot |\Delta H| \cdot \frac{T_a \cdot d_t^2}{4 \cdot \lambda_{er} \cdot T_w^2} \cdot \left(1 + \frac{8 \cdot \lambda_{er}}{U \cdot d_t}\right) < 0.4 \quad (2)$$

Calculations with typical values for a fixed bed of our Co/SiC extrudates operated in "classical" laboratory conditions ($\varepsilon = 0.4$; $r_p \approx 1.5\ \mathrm{mol_{CO}/m^3_{catalyst\ particles}/s}$; $T_a \approx 14{,}400$ K; $d_t = 2.54$ cm; $T_w \approx 493$ K; $\lambda_{er} \approx 1$ W/m/K and $U \approx 400$ W/m^2/K) gives a value

* Corresponding author.
E-mail address: regis.philippe@lgpc.cpe.fr (R. Philippe).

0920-5861/$ – see front matter © 2009 Elsevier B.V. All rights reserved.
doi:10.1016/j.cattod.2009.07.058

Nomenclature

Latin letters

ASM	mass specific activity of the catalyst ($g_{C_{5+}}/g_{cata}/h$)
ASV	volumetric specific activity of the catalyst ($g_{C_{5+}}/cm^3_{cata}/h$)
C_i	concentration of "i" specie (mol/m^3)
C_p	mass specific heat (J/kg/K)
d_p	average particle diameter of the extrudate catalyst (m)
$d_p^{éq}$	equivalent particle diameter of a foam catalyst (m)
d_t	tube diameter (m)
D_{er}	effective radial mass diffusion coefficient (m^2/s)
e_w	tube wall thickness (m)
h	heat exchange coefficient at the tube wall (W/m^2/K)
L	tube length (m)
M_i	molecular weight of "i" specie (kg/mol)
P	pressure (Pa or bar)
r	radial position (m)
$R_{réac}$	tube radius (m)
R	perfect gas constant: 8.314 (J/K/mol)
r_i	rate of consumption or apparition of "i" specie (mol/g_{cata}/s)
r_p	rate of reaction relatively to a catalyst particle volume (mol/$cc_{catalyst\ particle}$/s)
S_i	selectivity in "i" specie (mol%$_{CO\ converted\ in\ "i"}$)
T	temperature (K)
T_a	adiabatic temperature (=E_a/R) (K)
T_w	wall temperature (K)
U	global heat exchange coefficient at the tube wall (W/m^2/K)
u_s	superficial velocity of the fluid (m/s)
w_i	mass fraction of the "i" specie
WHSV	weighed hourly space velocity ($g_{CO+H_2}/g_{Co}/h$)
y_i	molar fraction of the "i" specie in the pseudo-phase
z	axial position in the tube (m)

Greek letters

α	growth probability factor used in the ASF theory
ΔH_j	heat of the "j"th reaction (J/mol)
ε	void fraction of the catalyst bed
λ	thermal conductivity (W/m/K)
μ	fluid viscosity (Pa s)
ξ	balance parameter used in the optimization function F
ρ	density (kg/m^3)
χ_i	molar conversion of "i" specie (mol%)

Subscripts and superscripts

0	inlet conditions
b	bulk
c	coolant
cata	catalyst bed
er	effective radial parameter
ext	wall at the coolant side
f	pseudo-fluid
i	specie "i"
int	wall at the pseudo-fluid side
j	"j"th reaction
p	catalyst particles

of 2.54 and this shows that radial temperature non-uniformities are much likely. That is why a 2D model is required to study the thermal role of the catalytic support in order to understand and improve heat removal in a catalytic tube.

2. Presentation of the model

2.1. Reactor

Because of the rough estimates of Mears criterion, a 2D model is required. Under typical low temperature FT condition (20 bar, 230 °C) more than 99 mol% of the reacting species are in the gaseous phase (thermodynamic equilibrium calculations), even though the process is aimed at producing waxes. Thus a gas–solid system can be assumed to estimate the main trends. Based on kinetic rate expressions given in the literature [4,5], it can be assumed that external mass transfer limitations can be neglected. Conversely, internal resistance can be significant [6], except when an egg-shell catalyst is used. This will be the assumption for the model presented below, which is of the pseudo-homogeneous type according to Froment and Bischoff [7]. In this steady-state model, a dispersive plug flow is described where mass and energy balances are identical in form: both are presenting an advective term, a radial dispersive term and a reactive term. The classical Ergun law rules correctly the momentum balance. Eqs. (3)–(5) summarize the governing equations and Eqs. (6)–(8) list the boundary conditions applied to one tube of the multi-tubular reactor. Fig. 1 gives a schematic view of one tube and a zoom in the wall region:

$$\rho_f \cdot u_s \cdot \frac{\partial w_i^f}{\partial z} = \rho_f \cdot D_{er} \cdot \left(\frac{\partial^2 w_i^f}{\partial r^2} + \frac{1}{r} \cdot \frac{\partial w_i^f}{\partial r} \right) + r_i \cdot M_i \cdot \rho_b^{cat} \tag{3}$$

$$\rho_f \cdot u_s \cdot C_p^f \cdot \frac{\partial T^f}{\partial z} = \lambda_{er} \cdot \left(\frac{\partial^2 T^f}{\partial r^2} + \frac{1}{r} \cdot \frac{\partial T^f}{\partial r} \right) + \rho_b^{cat} \cdot \sum_j r_j \cdot (-\Delta H_j) \tag{4}$$

$$-\frac{\partial P}{\partial z} = \frac{1-\varepsilon}{\varepsilon} \cdot \left(1.75 + 150 \cdot \frac{1\text{-}\varepsilon}{\mathrm{Re}} \right) \cdot \frac{\rho_f \cdot u_s^2}{d_p}$$

$$\text{with} \quad \mathrm{Re} = \frac{\rho_f \cdot u_s \cdot d_p}{\mu} \tag{5}$$

$$z = 0 : \forall r \, w_i^f = w_{i,0}^f; \qquad T_0^f = T_0^f \quad \text{and} \quad u_s = u_{s,0} \tag{6}$$

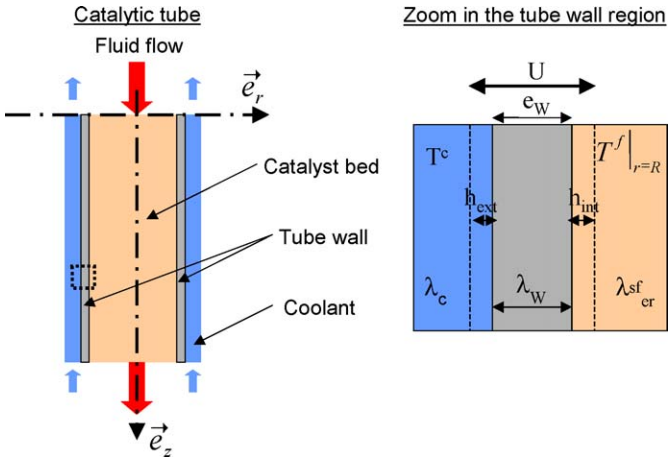

Fig. 1. Schematic view of a reactor tube with a zoom near the tube wall.

Table 1
Catalysts structural characteristics.

Catalysts	Bed density (kg/m$^3_{catalyst}$)	Mean particle diameter or equivalent diameter* (mm)	Bed void fraction	Cobalt content (wt%)
SiC foam	340	0.74*	0.88	30
SiC extrudates	950	1.00	0.40	30

* See Ref. [13].

$$r = 0 : \ \forall z \ \frac{\partial w_i^f}{\partial r} = \frac{\partial T^f}{\partial r} = 0 \tag{7}$$

$$r = R : \ \forall z \ \frac{\partial w_i^f}{\partial r} = 0 \quad \text{and} \quad \lambda_{er} \cdot \frac{\partial T^f}{\partial r} = U \cdot (T^f | - T^c)$$
$$\text{with} \quad \frac{1}{U} = \frac{1}{h_{ext}} + \frac{e_w}{\lambda_w} + \frac{1}{h_{int}} \tag{8}$$

For packed beds, thermal parameters used in the model (λ_{er} and U) are determined from classical correlations [8–11]. For monolithic foams, a specific correlation is used for λ_{er} determination [12] and in the absence of specific correlations, classical correlations proposed for spherical pellets are applied for U determination. Making use of the analogy of Lacroix et al. [13], the relevant size of the pellet is deduced from the geometric characteristics of the foam. The catalysts structural characteristics are listed in Table 1 and the thermal properties used in the correlations are listed in Table 2.

2.2. Kinetics

A simple semi-empirical kinetic model was adjusted on results obtained in a micro-pilot scale reactor (unpublished results). The objective of this kinetic model is to represent under industrially relevant situations the main trends of the chemical reactions according to the fluid composition and temperature which eventually depend on the physical properties of the catalyst (Al_2O_3/SiC, foam/particles). It is not a mechanistic description of the synthesis and no conclusion concerning catalyst formulation should be drawn from the results. Conversely, it is a good compromise between chemical description, mathematical tractability and industrial concerns that allows comparative studies. Kinetics experiments were performed using a monometallic cobalt catalyst supported on SiC extrudates and foams (200 °C < T_{inlet} < 250 °C; 20 bar < P_{inlet} < 40 bar; 10 wt% < Co content < 30 wt%; 0 mol% < inert gas fraction < 50 mol%; H_2/CO inlet molar ratio = 2.0; 0.2 $g_{syngas}/g_{catalyst}/h$ < weight hourly space velocity (WHSV) < 32.0 $g_{syngas}/g_{catalyst}/h$). A 1 in. i.d. stainless steel well-instrumented reactor was used. The kinetic model combines two expressions of rate laws from the literature to describe the CO conversion: Yates and Satterfield [14] expression is used for the Fischer–Tropsch synthesis and the Keyser et al. [15] expression for the water-gas shift reaction (WGS). This last law was derived from a Fe–Mn catalyst and it accounts for the effect of temperature and partial pressures of the reactants on the thermodynamic equilibrium of the WGS. The pre-exponential factor was adjusted on the results obtained with the Co catalyst, however the activation energy of Keyser et al. was used. The paraffin selectivity is described empirically. For the sake of simplicity, the model does not take into account olefins and oxygenates. Two specific laws are used for methane and ethane formation whereas for higher paraffinic products the recursive ASF theory of Anderson et al. [16] is applied using an average constant experimental coefficient α. The latter assumption may lead to a possible under-estimation of selectivity changes due to temperature changes. However, when comparing the effect of the catalyst support, the bias would be the very same and comparison would thus be meaningful.

The kinetic model contains five kinetic parameters that obey Arrhenius law. Activation energies are taken from literature data [14,15,17]. Eqs. (9)–(18) summarize the kinetic model used in this study:

$$r_{FT} = \frac{a \cdot \exp\left(\frac{-E_a}{R \cdot T}\right) \cdot C_{CO} \cdot C_{H_2}}{\left(1 + b \cdot \exp\left(\frac{-E_b}{R \cdot T}\right) \cdot C_{CO}\right)^2} \tag{9}$$

$$r_{WGS} = c \cdot \exp\left(\frac{-E_c}{R \cdot T}\right) \cdot \left(C_{CO} - \frac{C_{CO_2} \cdot C_{H_2}}{K_{WGS} \cdot C_{H_2O}}\right)$$
$$\text{with} \quad \ln(K_{WGS}) = \frac{2073}{T(\text{K})} - 2.029 \tag{10}$$

$$r_{CO} = -r_{FT} - r_{WGS} \tag{11}$$

$$r_{H_2O} = +r_{FT} - r_{WGS} \tag{12}$$

$$r_{CO_2} = +r_{WGS} \tag{13}$$

$$r_{C_1} = d \cdot \exp\left(\frac{-E_d}{R \cdot T}\right) \cdot r_{FT} \tag{14}$$

$$r_{C_2} = e \cdot \exp\left(\frac{-E_e}{R \cdot T}\right) \cdot r_{FT} \tag{15}$$

$$\text{For } n \geq 3 : \ r_{C_n} = \alpha \cdot r_{C_{n-1}} \tag{16}$$

$$\text{normalization in order to obtain} : \ r_{FT} = \sum_{i=1}^{N} i \cdot r_{C_i} \tag{17}$$

$$r_{H_2} = -r_{FT} + r_{WGS} - \sum_{i=1}^{N} (i+1) \cdot r_{C_i} \tag{18}$$

The exact reaction enthalpy of synthesis of a C_n (n = 1–50) paraffin is deduced from thermodynamic calculations. This is required for a reliable estimate of the heat generation and temperature profile in the reactor, and the impact on selectivity and productivity.

Parameters optimization (a, b, c, d and e) was made with a classical Levenberg–Marquardt algorithm, and the optimized parameters are given in Table 3. Fig. 2 shows the parity diagrams obtained for SiC foam and SiC pellet supports. Different kinetic parameters are obtained for SiC foams and SiC extrudates although it is the same Co active phase. This is due to different dispersions

Table 2
Thermal characteristics used in this study.

SiC porous support intrinsic thermal conductivity, λ_{SiC} (W/m/K)	Al_2O_3 porous support intrinsic thermal conductivity, $\lambda_{Al_2O_3}$ (W/m/K)	Average fluid thermal conductivity, λ_{f0} (W/m/K)	Wall thermal conductivity, λ_w (W/m/K)	Heat transfer coefficient at the tube wall on the coolant side, h_{ext} (W/m^2/K)	Tube wall thickness, e_w (mm)
4.0	1.0	0.2	60	1000	2.54

Table 3
List of kinetic parameters used in this study.

Support	a_0 ($m^6/mol/g_{cata}/s$)	E_a (kJ/mol)	b_0 (m^3/mol)	E_b (kJ/mol)	c_0 ($m^3/g_{cata}/s$)	E_c (kJ/mol)	d_0	E_d (kJ/mol)	e_0	E_e (kJ/mol)	α
SiC foams	3.42	100	0.45	20	14,527	145	1.94	81	1.087×10^{-4}	49	0.91
SiC extrudates	55.78		3.69		680,483		2.08		2.666×10^{-4}		0.80

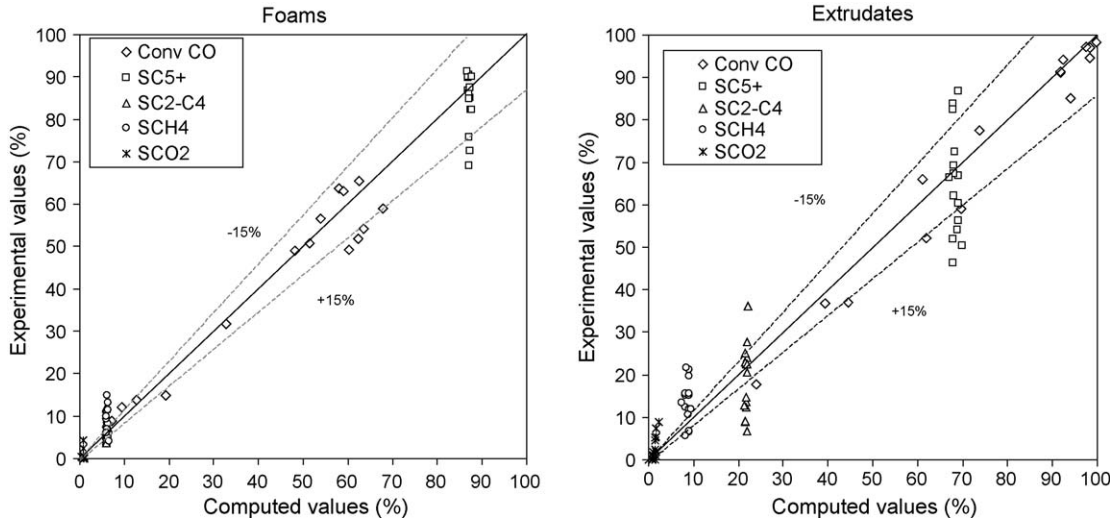

Fig. 2. Parity diagrams obtained for kinetic model optimization applied to the Co catalyst supported on SiC foam and extrudates.

and morphologies of the active phase and different pore distributions, specific surface areas and surface states owing to the synthesis process of each SiC structure and to the nature of the starting cobalt precursor. Conversely, to focus on the effects exclusively due to the thermal characteristics of the support, we use the same set of kinetic parameters both for SiC and Al_2O_3 supports (foam or pellets).

3. Results and discussion

The results presented below compare the performance of a reactor (given length and diameter of the single tube; see Table 4) packed with either a foam or an extruded catalyst made of alumina or SiC support. Because these catalysts have different densities and void fractions, the mass of catalyst per tube are different as well as the WHSV for given operating conditions.

3.1. Effect of intrinsic conductivity of the support and gas velocity for the two bed structures

Using a support of high thermal conductivity may be thought of interest for a better temperature control in FTS. Moreover, the continuous structure of a foam may seem attractive. Since radial heat transfer depends on axial velocity, we performed a sensitivity analysis of the reactor behaviour both on thermal conductivity of the matrix (alumina and silicon carbide) and superficial gas velocity. Figs. 3 and 4 represent respectively the evolution of effective thermal parameters of the bed and different reactor responses to variations in superficial velocity. The main simulated conditions are listed in Table 4.

For the pelleted and foam catalysts, when the superficial inlet gas velocity increases, λ_{er} and U are increasing due to a dominant convective contribution. For foams, the intrinsic thermal conductivity of the support do not affect significantly the global heat exchange coefficient U at the tube wall (Fig. 3). This results from the volumetric solid fraction which is smaller for a foam than for extrudates in a classical fixed bed. The global heat exchange coefficients for foams and extrudates are within the same range (300–550 $W/m^2/K$ depending on the velocity) and are always slightly higher for extrudates (all other parameters being identical). As far as effective thermal conductivity is concerned, it is logically observed that conductivities for SiC are higher than for Al_2O_3. The difference remains constant when the velocity increases. Both for pellets and foams, the difference between Al_2O_3 and SiC is almost constant and reflects the static contribution.

Concerning the hot spot amplitude (hot spot is defined as the highest simulated temperature in the tube), the CO conversion and the selectivity profile (Fig. 4), we observe that for high velocities (>0.15 m/s) there is no significant influence of the support: for a given catalyst structure (foam or pellets), conversions, hot spots and selectivity profiles are quite identical. For velocities lower than 0.15 m/s, the support exhibits a more marked thermal influence on selectivity and hot spot in the packed bed (Fig. 4, right column). With foams the hot spot difference is much smaller and no

Table 4
Main simulation characteristics.

d_{tube} (cm)	L_{tube} (m)	e_{tube} (cm)	$\varepsilon_{extrudates\ beds}$	d_p (mm)	ε_{foams}	$d_{p,\ éq\ foams}$ (mm)	$(H_2/CO)_{inlet}$ (mol/mol)	y_{inert} (mol%)	T_{inlet} (°C)	P_{inlet} (bar)	u_{inlet} (m/s)
2.54 → 4.06	11.9	0.254	0.40	1	0.88	0.724	1.9	22.2	220	31.4	0.003 → 0.447

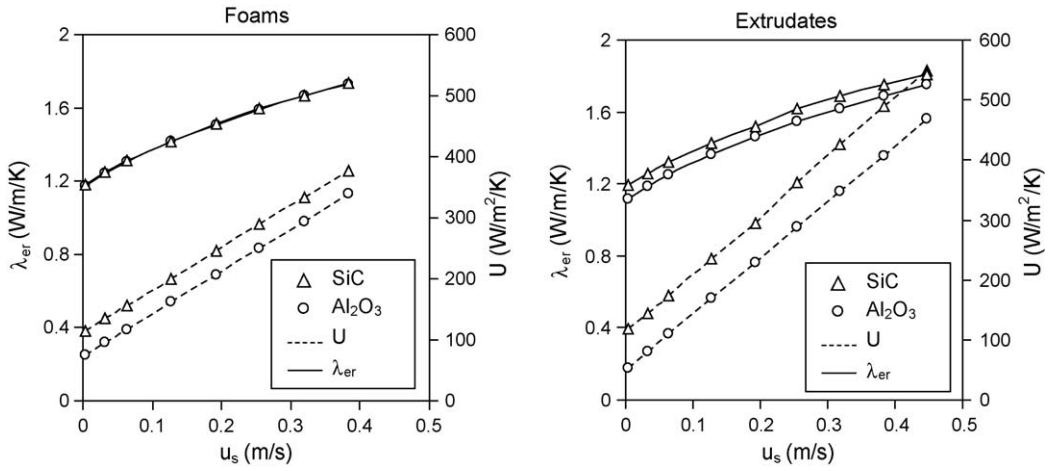

Fig. 3. Effect of thermal properties and inlet superficial velocity on the thermal coefficients: U and λ_{er}.

significant changes in selectivity are observed. This is essentially due to the smaller heat generated *per unit volume* of catalyst bed for foams than for extrudates owing to their higher void fraction. This points out the crucial importance of an appropriate tuning of the void fraction of the foam: the high porosity of a foam is beneficial from the point of view of heat removal and pressure drop, but this is at the expense of the volumetric productivity.

For both SiC supports, given the uncertainty about experimental hot spot location in the reactor, a quite good agreement has been observed between experimental and simulated hot spots and increases of temperature in the bed (comparisons shown in Fig. 5 made with kinetic experiments results). For alumina supports, the comparison is more hazardous.

3.2. Effect of intrinsic conductivity of the support and tube diameter for the two bed structures

Figs. 6 and 7 represent respectively the evolution of effective thermal parameters of the bed and different reactor responses for variations in tube inner diameter for alumina or silicon carbide structured as extrudates or foams. The main simulated conditions are identical to those given in Table 4, and the tube inner diameter

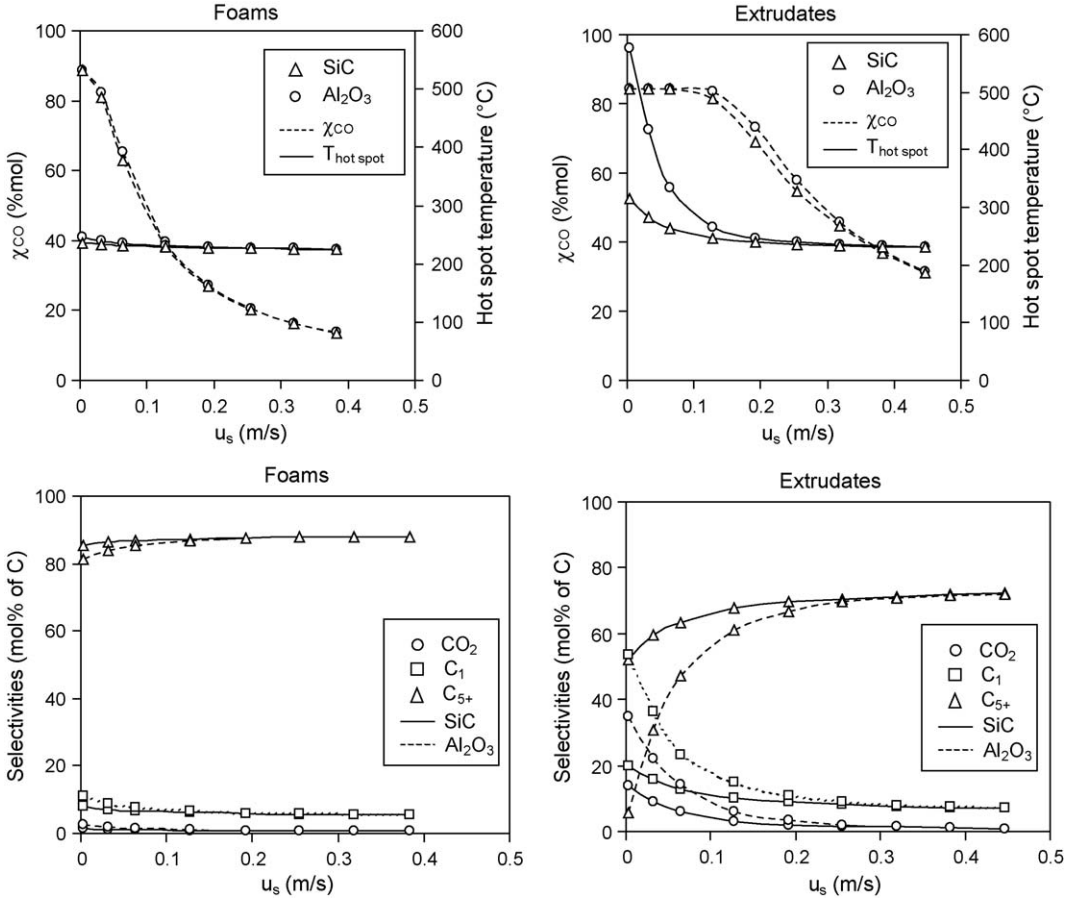

Fig. 4. Effect of thermal properties and inlet superficial velocity on the reactor performances: hot spot, conversion and selectivity profiles.

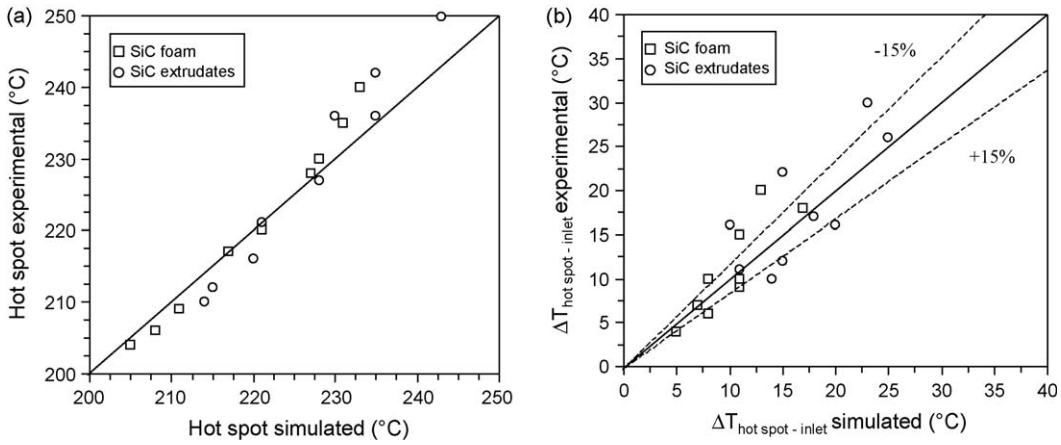

Fig. 5. Parity diagrams for (a) hot spot and (b) temperature increase inside the bed for SiC supports.

was varying from 2.032 cm (0.8 in.) to 4.064 cm (1.6 in.). The inlet velocity was kept at 0.255 m/s, i.e. a value which is typical of industrial reactors where the nature of the support is secondary as shown in the previous section.

For the two bed structures, when the tube diameter increases, λ_{er} increases slowly and U decreases (Fig. 6). For foams, these phenomena would be less pronounced than for extrudates. Moreover, as far as the nature of the support is concerned, the differences between SiC and Al_2O_3 are more pronounced with extrudates than with foams. These two results reflect again the smaller volumetric fraction of solid in a foam bed than in a packed bed. As expected, we observe for the two bed structures that an increase in tube diameter results in an increase in hot spot amplitude, CO conversion and a loss of selectivity (Fig. 7), owing to the smaller heat exchange surface area per unit volume at the wall of the tube. The support exhibits a more marked thermal influence with extrudates than with foams. Again, this behaviour is explained by the lower amount of heat generated per unit volume present in a foam than in a fixed bed of extrudates.

To summarize, the weaker sensitivity of foam beds to a reasonable tube diameter increase may be an advantage to decrease the number of tubes in parallel in a reactor with limited risk of thermal runaway. However, here again a tuning of the foam structure (i.e. porosity) is necessary to obtain the best compromise between catalytic activity and heat removal ability of the tube, for FTS or any other exothermic (or endothermic) catalytic reaction.

3.3. Summary of the results in terms of catalytic productivities towards C_{5+} species

Fig. 8 shows the simulated specific catalytic productivities – mass of C_{5+} species per unit time and unit volume (ASV) or mass of catalyst (ASM) – for both matrices and both structures. The evolution is plotted against the inlet superficial velocity (Fig. 8a) or the tube diameter (Fig. 8b). These specific productivities look like rates of reaction, however they involve the effect of the (possible) non-uniform temperature profile (radial and axial). They have thus no mechanistic meaning in general, whereas they are industrially meaningful.

We can see in Fig. 8a that foams are always exhibiting ASM quite higher than extrudates. This is mainly due to better intrinsic kinetics and selectivity encountered with foams (see Table 3). Conversely, and logically we observe that foams yields ASV lower than packed beds owing to the dominating effect of void fraction in a volumetric performance criterion. Nonetheless, it is interesting to see that for the lowest velocities ($u_s < 0.08$ m/s) foams exhibit ASV higher than extrudates. This is due to the huge differences encountered in hot spots and associated selectivity profiles with the two different catalytic structures at these velocities. As far as the material nature is concerned, no significant difference is observed between Al_2O_3 and SiC foams, this agrees well with the trends observed in the evolution of thermal parameters (Fig. 3). It can be noticed that within the range of simulated velocities, the Al_2O_3 foam exhibits always slightly higher performances than SiC.

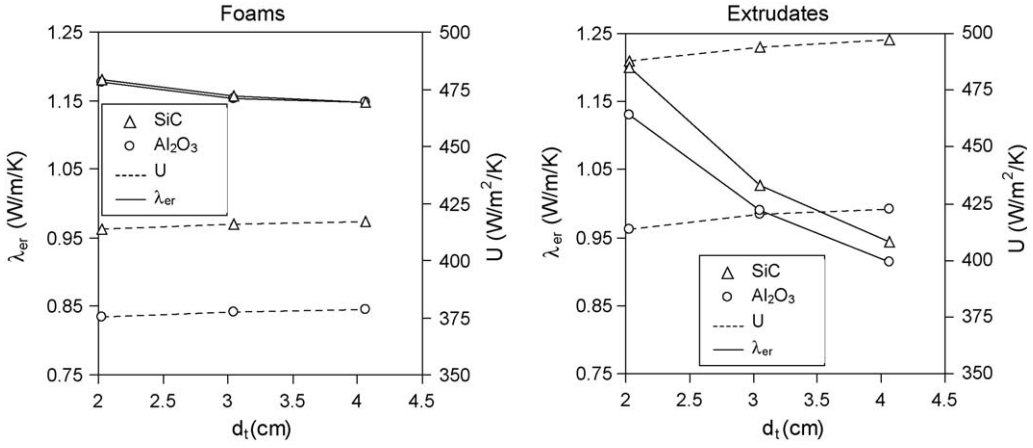

Fig. 6. Effect of thermal properties and tube diameter on the thermal coefficients: U and λ_{er}.

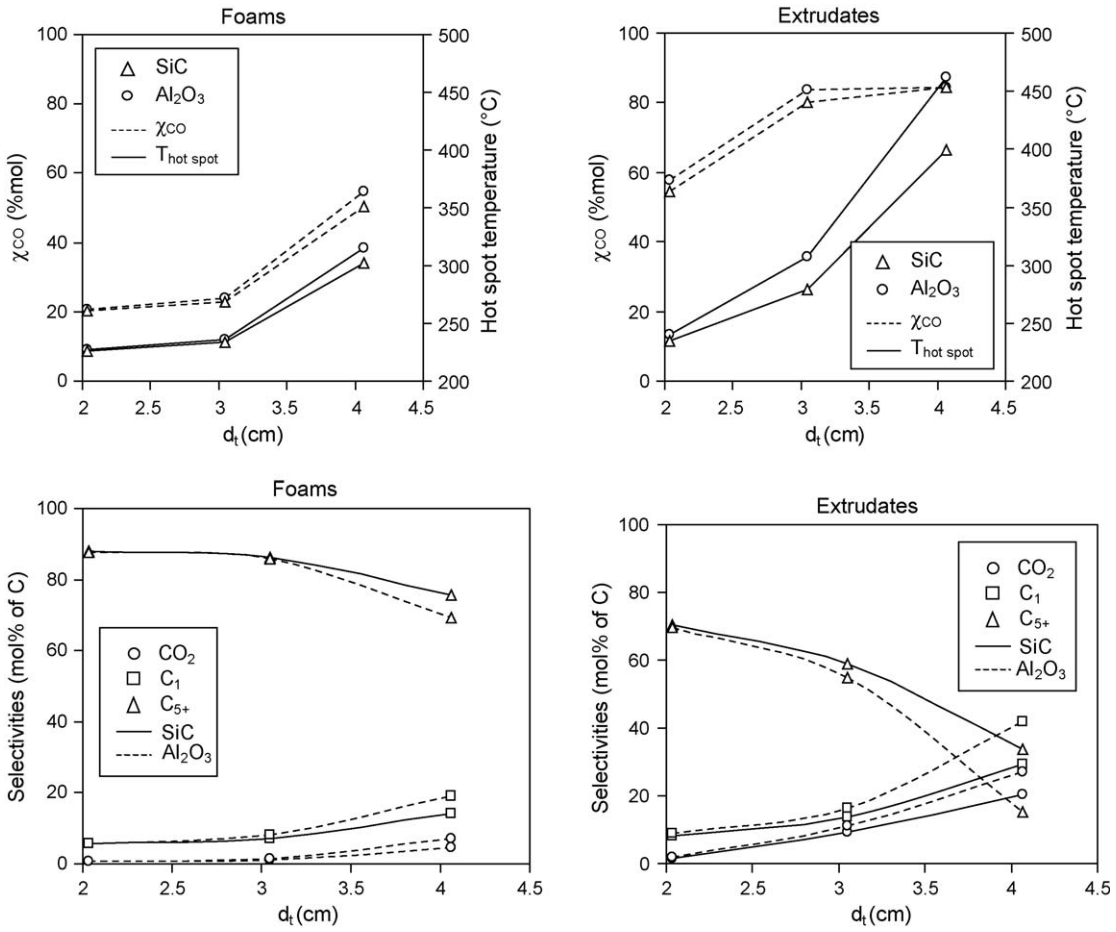

Fig. 7. Effect of thermal properties and tube diameter on the reactor performances: hot spot, conversion and selectivity profiles.

This behaviour reflects the lower intrinsic conductivity of the solid and the high void fraction of the bed that permit to reach bed temperatures high enough to boost the catalytic activity while preserving selectivity thanks to a still sufficient heat removal from the bed. For higher velocities (>0.2 m/s), the same trend is observed for the packed bed; but unlike foams, for the lowest velocities (<0.2 m/s) an inversion occurs and SiC extrudates exhibit better ASM and ASV than Al_2O_3. Al_2O_3 extrudates are submitted to higher hot spot amplitudes due to a weaker heat removal ability (see Fig. 3), and this leads to a dramatic decrease in C_{5+} selectivity (see Fig. 4) unbalanced by a gain in catalytic activity because we are in an experimental domain where CO conversion reached completion for both matrices.

Fig. 8b shows the evolution of the same specific catalytic productivities with tube diameter for both matrices and structures. The performances of the foam structures increase with tube diameter (within the range studied) whereas they decrease for extrudates (between 3.048 and 4.064 cm tube inner diameter).

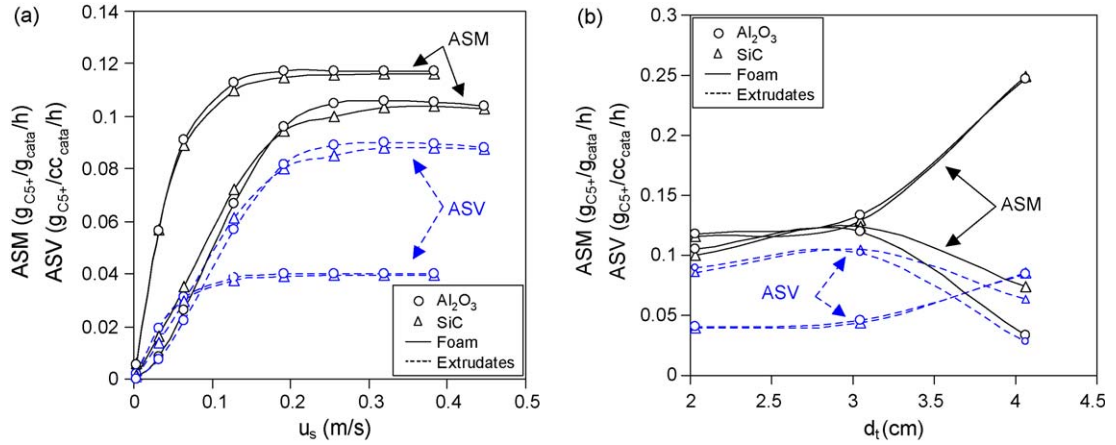

Fig. 8. Evolution of different specific catalytic activities (per unit volume and mass of catalytic bed) for (a) the velocity effect study and (b) the tube diameter effect study.

This phenomenon agrees with the hot spot and selectivity evolutions (Fig. 7): for both structures, the increase in tube diameter involves an increase in hot spot temperature and a decrease in selectivity towards C_{5+} species. Nonetheless, in the case of extrudate beds, the depletion is more pronounced and impacts badly the overall yield towards C_{5+} species.

As far as the nature of the support is concerned, Al_2O_3 becomes less efficient than SiC when the tube diameter increases, and this trend is again more significant with classical packed bed because of the higher amount of catalyst per unit volume of reactor. This agrees well with our previous comments about the increasing thermal role of the support when the tube diameter increases.

4. Conclusion

A fixed bed reactor model for FTS using a cobalt catalyst has been developed. This model allows investigations of the thermal properties of the catalyst support. We show that the intrinsic thermal conductivity of the support plays an important role in laboratory scale experiments where generally the fluid superficial velocity is very low (in the range of 10^{-4}–10^{-3} m/s). When industrial velocity conditions are considered (up to 0.5 m/s), the nature of the support becomes less important until being negligible. Nonetheless, at a given velocity when the tube diameter increases, the nature of the support becomes greater. Finally, in identical conditions, the use of a foam support instead of a classical bed packed with pellets seems to lead to a less pronounced effect of the support on the yield towards C_{5+} species and a better heat control. This is explained by the dilution of the heat generation in the bed volume due to the higher void fraction of foams. It is made at the expense of the catalytic activity *per unit volume* of reactor but it points out some interesting considerations about the tuning of the foam void fraction and of the reactor to ensure good heat exchanges in the bed and as high as possible volumetric activity of the foam catalyst. All these results are probably highly dependent on the contact between the foam and the reactor wall that governed the wall heat transfer coefficient. Convincing experimental results on this subject are still lacking. For further studies on thermal behaviour of foams under typical flow conditions of catalytic reactors, either one- or two-phase flow is necessary.

References

[1] B.H. Davis, Top. Catal. 32 (2005) 3.
[2] M.E. Dry, Appl. Catal. A: Gen. 276 (2004) 1.
[3] D.E. Mears, J. Catal. 20 (1971) 127.
[4] G.P. Van der Laan, A.A.C. Beenackers, Catal. Rev. Sci. Eng. 41 (1999) 255.
[5] B.W. Wojciechowski, Catal. Rev. Sci. Eng. 30 (1988) 629.
[6] X. Zhan, B.H. Davis, Appl. Catal. A: Gen. 236 (2002) 149.
[7] G.F. Froment, K.B. Bischoff, Chemical Reactor Analysis and Design, 2nd edition, J. Wiley & Sons, New York, 1990.
[8] F.W. Hennecke, E.U. Schlünder, Chem. Ing. Tech. 45 (1973) 277.
[9] R. Bauer, E.U. Schlünder, Int. Chem. Eng. 18 (1978) 181.
[10] R. Bauer, E.U. Schlünder, Int. Chem. Eng. 18 (1978) 189.
[11] E.U. Schlünder, P. Krötzsch, F.W. Hennecke, Chem. Ing. Tech. 42 (1970) 333.
[12] R. Singh, H.S. Kasana, Appl. Therm. Eng. 24 (2004) 1841.
[13] M. Lacroix, P. Nguyen, D. Schweich, C. Pham Huu, S. Savin-Poncet, D. Edouard, Chem. Eng. Sci. 62 (2007) 3259.
[14] I.C. Yates, C.N. Satterfield, Energy Fuels 5 (1991) 168.
[15] M.J. Keyser, R.C. Everson, R.L. Espinoza, Ind. Eng. Chem. Res. 39 (2000) 38.
[16] R.B. Anderson, R.A. Friedel, H.H. Storch, J. Chem. Phys. 19 (1951) 313.
[17] S. Storsaeter, D. Chen, A. Holmen, Surf. Sci. 600 (2006) 2051.